

# Combining lidar estimates of aboveground biomass and Landsat estimates of stand age for spatially extensive validation of modeled forest productivity

M.A. Lefsky<sup>a,\*</sup>, D.P. Turner<sup>b</sup>, M. Guzy<sup>b</sup>, W.B. Cohen<sup>c</sup>

<sup>a</sup>Department of Forest, Rangeland and Watershed Stewardship, Colorado State University, 131 Forestry Building, Fort Collins, CO 80523-1470, United States

<sup>b</sup>Department of Forest Science, Oregon State University, Corvallis, OR 97331, United States

<sup>c</sup>USDA Forest Service, Forestry Sciences Laboratory, Pacific Northwest Research Station, Corvallis, OR 97331, United States

Received 12 January 2004; received in revised form 27 December 2004; accepted 28 December 2004

## Abstract

Extensive estimates of forest productivity are required to understand the relationships between shifting land use, changing climate and carbon storage and fluxes. Aboveground net primary production of wood ( $NPP_{Aw}$ ) is a major component of total NPP and of net ecosystem production (NEP). Remote sensing of NPP and  $NPP_{Aw}$  is generally based on light use efficiency or process-based biogeochemistry models. However, validating these large area flux estimates remains a major challenge. In this study we develop an independent approach to estimating  $NPP_{Aw}$ , based on stand age and biomass, that could be implemented over a large area and used in validation efforts. Stand age is first mapped by iterative unsupervised classification of a multi-temporal sequence of images from a passive optical sensor (e.g. Landsat TM). Stand age is then cross-tabulated with estimates of stand height and aboveground biomass from lidar remote sensing.  $NPP_{Aw}$  is then calculated as the average increment in lidar-estimated biomass over the time period determined using change detection. In western Oregon, productivity estimates made using this method compared well with forest inventory estimates and were significantly different than estimates from a spatially distributed biogeochemistry model. The generality of the relationship between lidar-based canopy characteristics and stand biomass means that this approach could potentially be widely applicable to landscapes with stand replacing disturbance regimes, notably in regions where forest inventories are not routinely maintained.

© 2005 Elsevier Inc. All rights reserved.

**Keywords:** Lidar estimates; Aboveground biomass; Landsat

## 1. Introduction

Several alternative approaches have been employed for spatial scaling of net primary production (NPP) in forests. One approach relies heavily on remote sensing of  $f_{APAR}$  (the fraction of photosynthetically active radiation (PAR)

absorbed by the canopy). The combination of  $f_{APAR}$  and incident PAR is used to determine absorbed PAR (APAR) and a model based on light use efficiency converts APAR to NPP per unit area (e.g. Goetz et al., 1999). A second scaling approach relies on models that are more process-based and that are driven primarily by distributed meteorological data (e.g. Bachelet et al., 2003). Validation of scaled NPP products from both of these approaches has been limited. However, comparisons with independent measurements are needed to improve model parameterization and to further model development.

For the purposes of understanding the carbon cycle, estimation of aboveground wood production ( $NPP_{Aw}$ ) is

DOI's of original article: 10.1016/j.rse.2005.01.004, 10.1016/j.rse.2005.01.010.

\* Corresponding author.

E-mail addresses: [lefsky@cnr.colostate.edu](mailto:lefsky@cnr.colostate.edu) (M.A. Lefsky), [david.turner@oregonstate.edu](mailto:david.turner@oregonstate.edu) (D.P. Turner), [michael.guzy@oregonstate.edu](mailto:michael.guzy@oregonstate.edu) (M. Guzy), [warren.cohen@oregonstate.edu](mailto:warren.cohen@oregonstate.edu) (W.B. Cohen).

particularly important since  $NPP_{Aw}$  is often closely related to net ecosystem production (NEP, Curtis et al., 2002). This relationship of  $NPP_{Aw}$  to NEP is strongest in young stands but breaks down in recently disturbed stands where heterotrophic respiration is high, and in old stands where tree mortality tends to balance  $NPP_{Aw}$ . Some light use efficiency models, e.g. the 3-PG model (Landsberg & Waring, 1997), and most process-based models have allocation algorithms that isolate  $NPP_{Aw}$ . The difficulties in validating modeled  $NPP_{Aw}$  relate to both methodological issues with measurements of  $NPP_{Aw}$  and constraints on achieving a comprehensive sample of points over large spatial domains.

Measurement strategies have focused defining NPP as

$$NPP = \sum P_i + H_i$$

where  $P_i$  is the net production of dry biomass for plant tissue ( $i$ ) and  $H$  is the loss to herbivory (Gower et al., 1999). In temperate forests,  $NPP_{Aw}$  is commonly determined by an allometric method (e.g. Acker et al., 2002), wherein total stem biomass is estimated from allometric equations based on stem diameter, and  $NPP_{Aw}$  is estimated from the difference in stem biomass at two points in time. Some of the issues that arise include: evaluating the suitability of allometric equations, accounting for mortality, and ensuring continuity in the measurement protocols. With regard to devising the layout of sample points, critical issues include: achieving representativeness, optimizing sample locations to maximize access to existing roads, and minimizing spatial autocorrelation. In some cases, existing networks of permanent plots—such as the U.S. Forest Service Forest Inventory and Analysis (FIA) plots—have been used for  $NPP_{Aw}$  validation (Jenkins et al., 2001; Law et al., 2004), but are therefore limited to areas where such inventories are available.

In this study, we demonstrate the potential of integrated lidar and Landsat datasets for characterizing  $NPP_{Aw}$  over a spatially extensive set of plots (the lidar/change detection or LCD approach). We first developed a generalized relationship between forest canopy characteristics (estimated by lidar remote sensing) and tree biomass (calculated from field measurements). We then used multitemporal Landsat imagery (1972–1995) to determine stand ages up to 23 years over a large area of coniferous forest in western Oregon. A set of 407 plots was then identified by segmenting them from the portions of existing lidar flight lines that were coincident with areas of change.  $NPP_{Aw}$  was then calculated as the average increment in lidar-estimated biomass during stand development. Both the  $NPP_{Aw}$  and aboveground biomass estimates provide a basis for evaluating estimates of the same variables from a spatially distributed biogeochemistry model. Results were also compared to regional, age-specific,  $NPP_{Aw}$  estimates from FIA data.

## 2. Methods

### 2.1. A generalized canopy structure–biomass equation

To relate lidar estimates of canopy structure to field measurements of stand biomass, field data was collected in five study areas (Fig. 1). Plots were established along lidar transects, with plot locations based on the objective of achieving a range of stand ages and canopy structures.

#### 2.1.1. SLICER data collections

Lidar waveforms were collected by the SLICER (Scanning Lidar Imager of Canopies by Echo Recovery) instrument in September 1995 (Fig. 2). SLICER is a modified scanning version of a profiling laser altimeter developed at Goddard Space Flight Center (Blair et al., 1994). The SLICER system digitizes the entire height-varying return laser power signal, resulting in a waveform that records the reflection of light from multiple canopy elements (foliage and woody structure) over a large (5–10 m diameter) footprint, at the wavelength of the transmitted pulse (1064 nm). The lidar waveforms used in this work had a nominal footprint diameter of 10 m, and were collected in a swath that was 5 footprints wide (Lefsky et al., 1999a).

Georeferencing of lidar footprints is accomplished by combining laser ranging data with aircraft position, obtained via kinematic GPS methods, and laser pointing, obtained

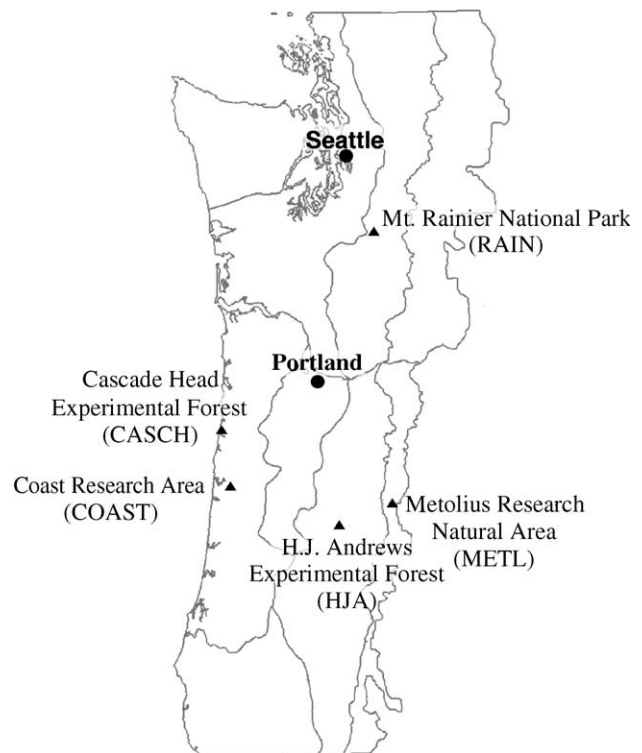


Fig. 1. Map of sampling areas used to create the unified equation relating lidar measurements to field estimates of aboveground biomass. A total of 87 plots were distributed in these five areas. The lines indicate ecoregion boundaries.

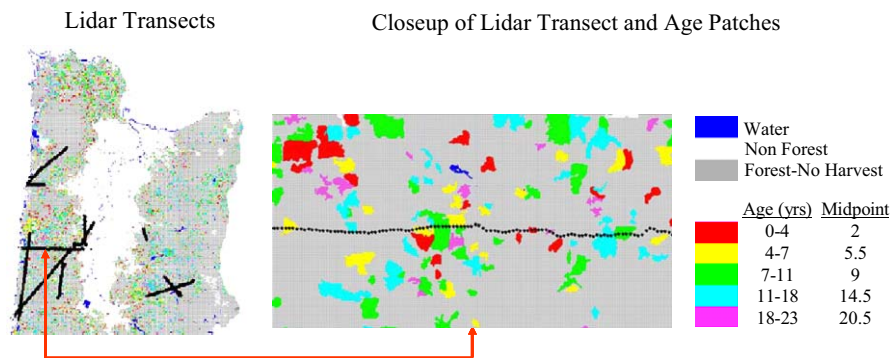


Fig. 2. Lidar transects and a sample of the mapped stand ages that are based on change detection analysis.

with a laser-ring gyro Inertial Navigation System mounted on the SLICER instrument (Blair et al., 1994). Georeferencing of the SLICER data used in this study was done at Goddard Space Flight Center using software developed by J. Bryan Blair. During the period in which these measurements were taken, the vertical resolution of the waveforms collected by SLICER was set at 11 cm, which when combined with the 600 vertical sample waveform, limited the waveform to a maximum height of 66 m. Due to additional constraints in the waveform processing software, all waveforms greater than 63 m have been truncated to 63 m. Given the tall stature of trees in Oregon and Washington forests (up to 75 m), the truncation problem affects about 3% of the waveforms used in these analyses. Ground returns on several footprints of old-growth plots had to be set by hand due to loss of the ground return as a consequence of the truncation error. Ground return positions were set based on the characteristics of adjacent footprints and independent estimates of topography (Means et al., 1999).

### 2.1.2. Field dataset

Field sampling was performed in 1996 at H.J. Andrews Experimental Forest (26 plots), in 1998 at the Metolious Research Natural Area (12 plots), in 1999 at the Cascade Head Experimental Forest (13 plots) and Coast study area (25 plots), and in 2000 at Mt. Rainier National Park (10 plots). Tree composition at these locations reflects climate and edaphic variability, potential vegetation type, and past and present management practices in Pacific Northwest forests (Franklin & Dyrness, 1988). Cascade Head, the most productive site, is dominated by *Picea sitchensis* (Sitka spruce) and *Tsuga heterophylla* (western hemlock). Both the Coast Range forest and H.J. Andrews sites are predominately *Pseudotsuga menziesii* (Douglas-fir), with significant *T. heterophylla* (western hemlock) at HJA, and abundant *Alnus rubra* (red alder) in the understory of the coastal forest. The plots at Mt. Rainier are all above 1300 m elevation and their composition is largely made up of a variety of “true” firs: *Abies amabilis* (Pacific silver fir), *Abies lasiocarpa* (sub-alpine fir), and *Abies procera* (noble fir) as well a number of other species, including

*Chameocyparis nootkatensis* (Alaskan cedar), *T. heterophylla*, and *T. mertensiana* (mountain hemlock). The Metolious Research Natural Area on the east side of the Cascade Range near Sisters, Oregon, is dominated by *Pinus ponderosa* (Ponderosa Pine), which accounts for 88% of basal area.

Eighty-four 0.25 ha field plots were established under existing SLICER transects using locations determined using differentially corrected GPS (Global Positioning System) receivers. At each plot a 50-by-50 m plot was oriented with the bearing of the SLICER transect, and laid out with dimensions corrected for slope. The intensity of field sampling was a function of stand structure. On old-growth plots all trees greater than 1.37 m tall were measured. On young and mature plots where tree densities were higher, all trees greater than 1.37 m tall were measured on subplots. Tree diameters were initially measured on 3 or 5 subplots, each 10 m in diameter. Then the number of additional subplots (5, 9, or 13) needed to sample at least 30 dominant and codominant trees was estimated and regularly spaced to cover the full extent of the plot. In each subplot, all trees greater than breast height (1.37 m), species, diameter at breast height, and crown ratio (the proportion of the bole with live crown) were recorded. More details on field data collection and processing can be found in Lefsky et al. (1999a).

Total aboveground biomass (AGBM) was estimated from DBH and height using allometric equations generated from a dataset of tree volume collected in 18 different protected areas and experimental forests throughout the Pacific Northwest and Colorado (Franklin, 2002). Site productivity has a significant effect on the allometric relations between tree height and DBH, and as a consequence, AGBM and DBH. The Schumacher equation (Schumacher & Hall, 1933) was adopted to reduce the impact of site productivity on estimates of aboveground biomass at each site. The Schumacher equation uses both the height and diameter of trees to predict stem volume, or when wood density is considered, stem biomass. Because trees in high productivity locations are taller, in general, for a given diameter, they will also

have higher volume and biomass than trees of the same diameter on lower productivity sites. Therefore equations based on DBH alone may be biased when applied at sites of varying productivity. Wood and bark densities were taken from USDA Forest Products Laboratory's Wood Handbook (USDA Forest Products Laboratory, 1999). As in Lefsky et al. (2005a) an additional 10% was added to the bole biomass to account for branch biomass, which along with bole biomass provides aboveground woody biomass.

To utilize these equations, estimates of height and DBH are required for every tree. Measuring the height of each individual tree was not feasible for all 11280 trees sampled in this study; the heights of 1096 trees were measured using a laser rangefinder. The height of trees that did not have measured heights was estimated using an imputation procedure (Lefsky et al., 2005a; Moeur & Stage, 1995) and allometric equations based on the Schumacher equation were used to compute aboveground biomass for each tree (Lefsky et al., 2005a).

### 2.1.3. Lidar processing

We used the 84 field plots for the development of canopy structure–biomass regression equations. Sixty-four of the field plots (76%) had 25 waveforms (collected as a five-by-five array). Six of the 19 plots that had less than 25 waveforms were at the Mt. Rainier site. These plots are all found where varying aircraft speed led to the distance between waveforms being stretched in the direction of flight, changing the number of waveform footprints that fit within the standard 50 m×50 m sampling plots. For one plot at the COAST site and two plots at the HJA site, we sampled conditions that were less than 50 m×50 m in size, and therefore we used a subset that was smaller than 25 waveforms. This was due to a need to obtain certain forest conditions that were only available in patches less than the standard size. The remaining 10 plots are all located at the Metolius site, where the fine grained spatial pattern of the ponderosa pine stands meant that a 50×50 plot would have encompassed a wide variety of stand conditions, and so between 5 and 23 waveforms (12 on average) defined a plot.

In a waveform-recording system such as SLICER, the height of the canopy is measured as the vertical distance between the elevation of the first return energy and the elevation of the peak of the ground return. The elevation of the first return energy is the point at which the power of the reflected light exceeds a threshold value; passing this threshold triggers the sensor's waveform recording process. The position of the peak of the ground return is calculated using the IMH (Interactive MacArthur-Horn) waveform processing software (Harding et al., 2001). The mean canopy height is then calculated for all the waveforms coincident with a stand.

A second variable used in this work is based on the calculation of the canopy height profile (CHP) which is a

modification of the foliage height profile or FHP (MacArthur & Horn, 1969). The FHP quantifies the distribution of foliage surface area as a function of height. Because SLICER cannot distinguish woody surface area and foliage surface area, the CHP is defined as the distribution of both foliar and woody surface area as a function of height. One measurement made using CHPs is the quadratic mean canopy height which is calculated as the mean of the canopy height profile weighted by the squared height of each element. This variable has been shown to be valuable in the prediction of stand characteristics in an eastern deciduous forest (Lefsky et al., 1999b). In this work, the standard deviation of each of the quadratic mean canopy heights associated with a plot is used as an estimate of canopy variability.

The third variable used in this work is the oligophotic volume, which is derived from the canopy volume method (CVM, Lefsky et al., 1999a). This method is explicitly volumetric as it uses a grid of contiguous lidar waveforms (e.g. 5×5 horizontal footprints) to characterize the forest canopy as a three-dimensional array. Oligophotic volume is the volume of space that is filled with foliage and woody biomass but which is below the height at which 65% of the lidar signal has been returned to the sensor—a proxy for shaded lighting conditions. Oligophotic volume is, therefore, the estimated volume of shaded foliage and woody material within the canopy.

Lefsky et al. (1999a) and Lefsky et al. (2005b) fully describe these canopy structure indices, and the mechanisms relating them to aboveground biomass. Estimates of these indices of canopy structure from SLICER were transformed into estimates of aboveground biomass using a single equation derived from analysis of data collected on the 87 field plots. Stepwise multiple regression was used to develop the following equation relating lidar estimates of forest canopy structure and field estimates of aboveground biomass (Fig. 3):

$$\text{AGBM} = 4.236 + 0.200 \cdot \text{CHP\_H\_X}^2 + 13.325 \cdot \text{OLIGO} + 24.300 \cdot \text{CHP\_Q\_SD} \quad (1)$$

where AGBM units are Mg ha<sup>-1</sup>, CHP\_H\_X<sup>2</sup> is the mean height of the forest canopy (m), squared, OLIGO is the volume of shaded foliage and woody biomass in the canopy (m<sup>3</sup>), and CHP\_Q\_SD is the standard deviation of the quadratic mean height of the canopy (m).

The R<sup>2</sup> of the equation is 87% (P<0.0001), the RMSE is 118.5 Mg ha<sup>-1</sup>. When regressions between predicted and observed AGBM were performed for individual study sites, none of the resulting regressions showed significant differences between their slopes and intercepts and those expected with a identity relationship (e.g. Intercept=0, Slope=1). The relationship was then applied to the total lidar dataset by segmenting the lidar footprints into 5×5, non-overlapping, arrays of data, processing the data to produce estimates of canopy structure indices for the entire

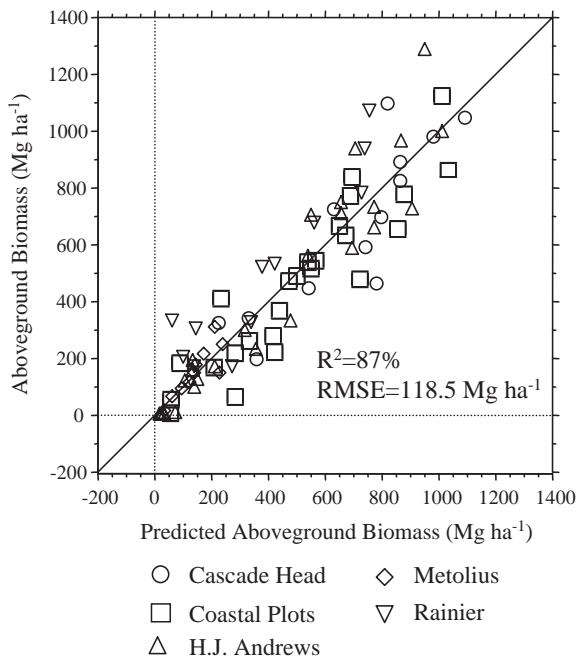


Fig. 3. Predicted and observed aboveground biomass for plots at the five sampling areas in western Oregon and Washington. This relationship explains 87% of variance, and none of the five areas showed significant differences in their slopes or intercepts from the overall equation.

dataset, and then using the above equation to create estimates of aboveground biomass, as well as well canopy height.

## 2.2. Determining stand age

A time series of Landsat images was used to estimate the ages of all stands disturbed between 1972 and 1995. This is possible because, in this region, stand replacement disturbance has a strong and distinct spectral signal in Landsat data (Cohen et al., 1998). Stand age at the time of the SLICER flights was determined as the difference between the year of the SLICER flights (1995) and the midpoint of the time period in which stand replacement occurred. Estimates of stand age from image processing used in this paper were developed and verified by Cohen et al. (1998, 2002), and their methods are only briefly described here. The images used are from the Landsat satellite; the earlier dates are from the Multispectral Scanner (MSS) sensor and the latter are from the Thematic Mapper (TM) sensor. Cohen et al. (2002) selected the years 1972, 1977, 1984, 1991 and 1995 as target years from image processing, although in some cases, good quality images from these year were not available and images from adjacent years were used. As in Cohen et al. (1998), each individual MSS and TM image was transformed into Tasseled Cap brightness and greenness vegetation indexes (Crist & Cicone, 1984; Kauth & Thomas, 1976), and for TM images, the Tasseled Cap wetness index, for a total of 15 spectral bands. A

georeferenced mosaic of images from 1988 was developed; all images from the other dates were georeferenced to this mosaic. There were radiometric differences among the images in both space and time, but the noise associated with temporal radiometric differences is minimal relative to the signal from stand replacement forest disturbance (Cohen et al., 1998).

This method follows a prototype disturbance detection exercise reported by Cohen et al. (1998) and a conceptual examination of change detection algorithms by Cohen and Fiorella (1998). First, an unsupervised classification is performed on a full stack of 15 Tasseled Cap indices. Unsupervised clustering was an iterative process whereby individual image pixels were labeled as “disturbed” (by time period), “undisturbed,” or “confused.” “Confused” pixels were reclustered several times until all pixels could be confidently labeled as “disturbed” or “undisturbed.” The resulting map was subjected to two additional processes for further refinement. The first was to relabel all nonforest land-use areas as nonforest, using a zoning data layer available through the Oregon State Services Center for GIS. The second process was to “smooth” all patches within the forest class (both disturbed and undisturbed) using a  $3 \times 3$  majority filter and then merge all patches less than 2 ha with surrounding patches that were larger than 2 ha. The rule set used allowed all patches of forest disturbed during different time intervals to be merged prior to any mergers of disturbed and undisturbed forest. Fig. 2 illustrates the intersection of a lidar transect with the ages of patches defined by the multi-temporal image analysis.

## 2.3. Estimation of $NPP_{Aw}$ from lidar and Landsat

For segments of the SLICER transects that were identified as disturbed by the Landsat change detection, AGBM was calculated and averaged.  $NPP_{Aw}$  was then calculated as the rate of increase in the average AGBM that occurred between two time periods. Originally the two time periods used were the youngest and oldest but, due to biases in the earliest years’ AGBM estimates, the 14.5 and 20.5 age-classes were used for subsequent analysis. During the first years of succession, the change in foliar biomass is minimal relative to the change in woody biomass so our  $NPP_{Aw}$  is effectively mean annual wood production over the life of the stand. Note that formally, mean annual increment (MAI) is based specifically on the age at maximum annual increment (Hanson et al., 2002), but that here the reference age is set by the change detection analysis.

## 2.4. Estimation of $NPP_{Aw}$ with Biome-BGC

Biome-BGC is a daily time-step biogeochemistry model with physiologically based algorithms for photosynthesis, autotrophic respiration and heterotrophic respiration (Running & Hunt, 1993; Thornton, 1998; Thornton et al., 2002).

For the purposes of scaling NPP or its components such as  $NPP_{Aw}$  over a region, the model is run cell-by-cell over a grid covering the area of interest. Model inputs for this study included distributed meteorological data from an 18-year daily climatology for the PNW region at a 1-km resolution, developed from the DAYMET model (Thornton et al., 2000, 1997; Thornton & Running, 1999).

The general procedures for application and validation of Biome-BGC in the Pacific Northwest (PNW) region have been reported elsewhere (Law et al., 2004; Turner et al., 2003, 2004a). The major carbon compartments, or pools, in the model include leaves and fine roots, as well as bole, coarse roots, coarse woody debris (CWD), litter and two classes of soil organic matter. To establish the initial conditions for those pools, a model “spin-up” is run. The soil carbon pools are brought into approximate equilibrium with the local climate during this thousand-year model run. In the spin-up, a multi-year climate time series is run repeatedly. Because most stands in the PNW region originated from catastrophic disturbances (Wallin et al., 1996), i.e. fire or logging, two successive disturbances are simulated at the end of each spin-up. The model was then run forward to the stand age specified by the change detection analysis. Then the Biome-BGC estimate of aboveground biomass associated with each disturbed plot along the lidar transect (407 plots) was isolated and  $NPP_{Aw}$  was determined from stand age and biomass. No attempt was made to correct for the difference in spatial resolution between the 1 km spatial resolution of BIOME-BGC model and the 50 m resolution of the SLICER data; a direct comparison were made between each dataset.

### 2.5. Estimation of biomass and NPP from forest inventory data

To serve as a third source of biomass and  $NPP_{Aw}$  estimates, plot-level data collected by the USDA Forest Service Forest Inventory and Analysis (FIA) program (USDA Forest Service Forest Inventory and Analysis, 1992) and the Forest Service’s Current Vegetation Survey were obtained for western Oregon. These two surveys cover the majority of forested lands, both private and public, although they exclude the small amount of forest on BLM lands in western Oregon. Inventory methods vary, but plots averaged about 1 ha in area. The species and diameter of each tree with a diameter at breast height greater than 2.54 cm were sampled on 1–10 nested fixed or variable-radius plots, and height was measured on a sub-sample of the trees (Ohmann & Gregory, 2002). As with the field data from lidar calibration plots, the heights of trees that did not have measured heights were estimated using an imputation procedure (Lefsky et al., 2005a; Moeur & Stage, 1995), and allometric equations based on the Schumacher equation (Lefsky et al., submitted for publication-a) were used to compute aboveground biomass

for each tree. Ages for the forest inventory plots are defined using the age-at-breast height information collected by the inventory. The FIA plots were aggregated into age class bins for the purposes of comparisons with the age classes based on change detection, and  $NPP_{Aw}$  was calculated in the same manner as for the lidar estimates of aboveground biomass.

### 3. Results

Across all segments in the lidar transects, the mean rate of canopy height growth increased nonlinearly with age (Fig. 4), and mean canopy height reached 11.5 m in the oldest age class (20.5 years). The relationship of lidar predictions of AGBM for all plots against AGBM estimated by Biome-BGC shows that Biome-BGC estimates (Fig. 5) are lower, particularly at low values, but are well correlated ( $R^2=64\%$ ). There are likely a number of reasons that the relationship is not stronger. First the ages of disturbed stands were estimated as the midpoint of each ~5 year interval. Second BGC estimates are based on a complex physiological model that may be inexactly parameterized and formulated. Thirdly, both sets of estimates are based on non-linear allometric equations that are by nature somewhat generalized. Finally, in the earliest age-classes there is a small positive offset in the lidar estimates of aboveground biomass (~22 Mg ha<sup>-1</sup>), due to the lidar device over-estimating the height of the trees in the smallest stands—probably a result of the presence of snags, stumps, etc., that cause an over estimation of stand height.

The mean aboveground biomass for each of the age classes, as predicted using lidar and Biome-BGC showed a similar pattern of increase with stand age. For the first two age classes the inventory estimates were between those from lidar and BGC, but were highest for the oldest 3 age classes. In all age-classes, the estimates are within a 20–30 Mg ha<sup>-1</sup> range. Differences between the inventory results and lidar estimates are partially related to the spatial

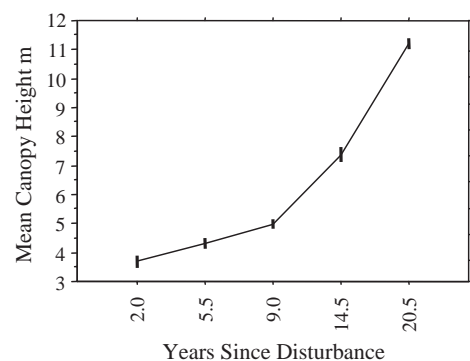


Fig. 4. Mean canopy height derived from lidar measurements as a function of years since disturbance. Error bars indicate one standard error.

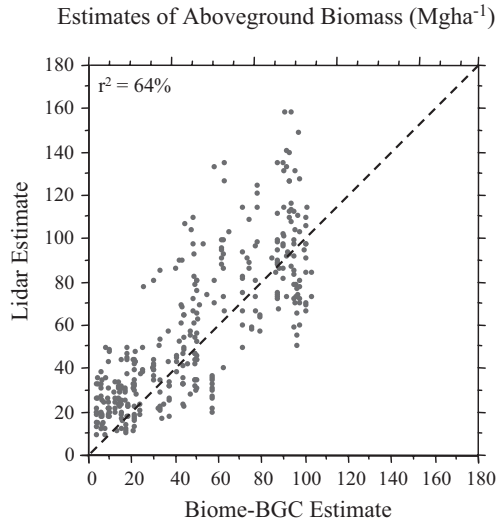


Fig. 5. Comparison of aboveground biomass ( $\text{Mg ha}^{-1}$ ) estimated from lidar/change detection and from Biome-BGC.

limitation of the lidar transects relative to the inventory data. Calculation of regional mean  $\text{NPP}_{\text{Aw}}$  was performed using the oldest age classes (ages 14.5–20.5), due to the lidar method’s higher estimates of aboveground biomass for the earlier age classes that were noted before (e.g. presence of stumps and small trees in early succession plots). The calculation resulted in the following estimates:  $6.7 \text{ Mg ha}^{-1} \text{ year}^{-1}$  for the LCD approach,  $6.8 \text{ Mg ha}^{-1} \text{ year}^{-1}$  for Biome-BGC, and  $7.2 \text{ Mg ha}^{-1} \text{ year}^{-1}$  for the inventory approach.

We also tested the ability of this  $\text{NPP}_{\text{Aw}}$  method to measure variability in productivity. To define productivity classes, the Biome-BGC estimates of final plot biomass were used to classify each patch into either high productivity (above mean biomass) or low productivity (below mean biomass). Both the Biome-BGC and lidar estimates of biomass were plotted as in Fig. 6, but split into high and low classes on the basis of the Biome-BGC productivity classes (Fig. 7). At 20.5 years, the difference between high and low

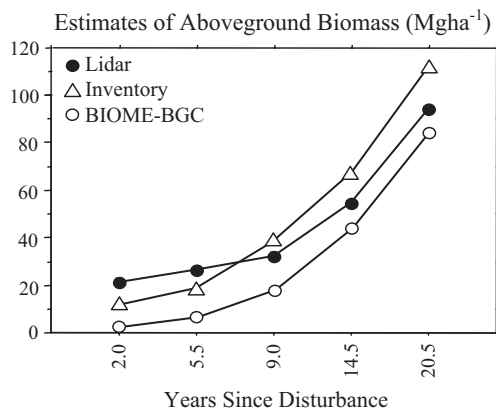


Fig. 6. Estimates of aboveground biomass ( $\text{Mg ha}^{-1}$ ) as a function of years since disturbance, from three methods: lidar predictions, Biome-BGC model results, and forest inventory plots.

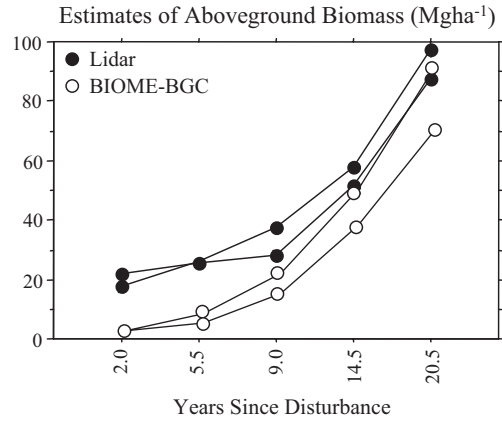


Fig. 7. Estimates of aboveground biomass ( $\text{Mg ha}^{-1}$ ) as a function of years since disturbance, for two methods: lidar predictions and Biome-BGC model results. Results from each method have been split into two classes: above and below the 50th percentile aboveground biomass value for each dataset.

productivity estimates from lidar is  $\sim 10 \text{ Mg ha}^{-1}$ , while the difference between high and low estimates from Biome-BGC was  $\sim 20 \text{ Mg ha}^{-1}$ .

#### 4. Discussion

The method presented here for estimating  $\text{NPP}_{\text{Aw}}$  may be widely applicable. It requires only that, over the area of interest, a significant number of patches have undergone stand replacement disturbance of a type that can be mapped with confidence. In some high productivity areas, distinguishing even very young stands may be difficult (Nelson et al., 2000), although high temporal resolution for the change detection may be one way to circumvent this problem. Regions in which clearcutting is the dominant mode of forest harvest would be particularly suitable. In areas with high cloud cover, such as some tropical areas, obtaining lidar and multi-temporal coverage of stand disturbance may be difficult (Asner, 2001). However, this method allows considerable flexibility in image selection, both in terms of the time of year, and the year of coverage. The year of coverage can be shifted by multiple years, as long as the year of coverage of individual multi-temporal stacks of images are recorded, and the years of the other images are shifted to avoid having too large a time interval. The time interval used in this study ( $\sim 5$  years) is fairly coarse; an interval of 1–3 years would help in reducing the error in the aboveground biomass (and therefore  $\text{NPP}_{\text{Aw}}$ ) estimates.

This method also requires the availability of an adequate number of lidar observations coincident with the disturbed patches, and that a relationship between lidar measurements of canopy height and aboveground biomass is available for the area in question. The former requirement could be met either by airborne lidar collections over a large area (as in this work, but preferably with more systematic sampling) or from spaceborne lidar with systematic sampling of a large landscape. Predicting aboveground biomass from lidar-

measured canopy height has now been shown to be straightforward exercise in a variety of forested biomes, and physiognomic types (Drake et al., 2002; Lefsky et al., 1999a, 1999b). In addition, it has now been shown that height-to-biomass relationships are quite stable among contrasting biomes (Lefsky et al., 2002) and among sites of different productivities within a biome (Lefsky et al., 2005b). Nevertheless, local calibration of these relationships would be desirable.

Because the satellite record extends back only to 1972 (with the launch of the first Earth Resources Technology Satellite, later renamed Landsat), the LCD approach to estimating  $NPP_{Aw}$  is currently restricted to the first 30 years or so of stand development. When and if a spaceborne lidar sensor with the ability to accurately measure canopy height is deployed, the potential will exist for extensive coverage of the land. As the lidar record is extended and disturbed sites begin to be revisited, it will also be possible to begin estimating the periodic annual wood increment (PAI) rather than the MAI (e.g. on a decadal scale). NPP and  $NPP_{Aw}$  generally increase in early succession and achieve their maximum values approximately when LAI is at its maximum (Ryan et al., 1997). Declines in  $NPP_{Aw}$  in older stands are often on the order of 50% (Acker et al., 2002; Gower et al., 1999). The periodic annual increment would be most relevant to validation of light use efficiency and process-based models driven by the LAI/fAPAR and climate observed from the same period.

In this study, the results for the 14–20 year old stands were most reliable; noise associated with residual vegetation left after disturbance introduces error on the younger sites. Note, however, that in terms of estimating the actual  $NPP_{Aw}$  this method would have a low bias that would increase with stand age. The issue here is that an estimate of  $NPP_{Aw}$  based on differences in total live biomass misses the effects of mortality. Field measurements of  $NPP_{Aw}$  based on resurveys of permanent plots usually track each tree and can thus either count production tree by tree, in which case mortality can be ignored, or account for the effects of mortality if estimating  $NPP_{Aw}$  by difference in total biomass. The mortality term is a small proportion of  $NPP_{Aw}$  (calculated by difference in total biomass) in a young stand but can be quite large in old stands (Acker et al., 2002); although the length of the satellite record is not yet long enough to include these old stands.

A primary advantage of the LCD approach to validation of models used for modeling NPP is its potential to be spatially extensive. Because of the significant resource requirements for measuring NPP (Clark et al., 2001), and the significant scaling issues associated with the local heterogeneity and the mismatch in scale between the coarse resolution of the satellite-based NPP estimates (e.g. 1 km) and the fine resolution at which NPP measurements are made (e.g. 25 m plots), efforts to validate the NPP estimates from the AVHRR and MODIS sensors have been quite limited (Running et al., 1999;

Turner et al., 2004b). When process-based models are used in the development of validation data, the LCD approach could help in model calibration and validation. In this study, we found an apparent underestimation of  $NPP_{Aw}$  from the Biome-BGC model runs; this could potentially be addressed by efforts to refine model parameterization. A notable virtue of the LCD approach is that it requires little or no historical data collection, thus extending validation efforts to forest areas that do not have established forest inventory programs.

Besides identifying possible overall estimation errors in model output, the LCD approach also potentially gives information on model sensitivity to environmental variation. The spatially varying inputs to Biome BGC include soil properties, as well as climate variables that could be formulated as climate indices, e.g. growing season precipitation. Plots of residuals in the LCD vs. model-based approach against these spatially varying inputs could help isolate particular weaknesses in model algorithms that might be the focus of further model development.

In using mean values for different age classes to estimate mean regional  $NPP_{Aw}$  by age class, this study suffers from the usual limitations associated with a space-for-time study design. This type of analysis typically is successful when the effect of particular historic events is small relative to the overall historic trend, and fails when historic effects are large (Pickett, 1989). In this case, aboveground biomass in any one time period is treated as if it is independent of the particular time period of stand initiation. It could be that the climatic conditions that were prevalent during one period would lead to variations in stand initiation that could affect aboveground biomass. However, the biomass of these stands are related to the accumulated climatic effects that were prevalent during (in the case of the periods used for the regional  $NPP_{Aw}$  analysis) the first 14.5 to 20.5 year of stand development, and those stands had 14.5 years in common. While this does not rule out the possibility of variations in productivity due to climatic effects, it should minimize those effects.

More troubling is the possibility that the population of stands that were disturbed in the 14.5 year old age class is fundamentally different from those stands being disturbed in the 20.5 year old age class. If, as in this landscape, logging is the primary disturbance, these activities may move from high productivity sites to low productivity sites or from publicly managed lands to privately managed lands. If, for instance, logging did progress from easily accessible, high productivity sites in the lowlands to higher altitude, lower productivity sites along hill slopes, the difference between older and younger stands is likely to be overstated, resulting in an overestimate of  $NPP_{Aw}$ . Therefore, knowledge of the disturbance and climatic history of an area, along with explicit analysis of the spatial distribution of disturbance, is desirable in using the LCD approach.

Pickett (1989) notes that space-for-time studies and more rigorous short- or long-term analyses are not mutually

exclusive. In fact, a simple complementary analysis using lidar to estimate productivity is possible using a modified design in which a small number of plots are followed up with a second set of lidar observations, spatially coincident with the first set, but taken 3–5 years later. In this case,  $NPP_{Aw}$  could be directly estimated using separate above-ground biomass estimates for each date, and then compared to  $NPP_{Aw}$  estimates from the space for time age class sequence based on the regional set of points.

Because lidar is effective at quantifying LAI and leaf biomass (Lefsky et al., 1999a), there is also the possibility of adding an estimate of foliage production ( $NPP_f$ ) to  $NPP_{Aw}$ . In a deciduous forest,  $NPP_f$  is simply the foliar biomass. In evergreen forests, the situation is more complicated because foliage retention time (FRT) may vary among species and age classes (Reich et al., 1995). However, generalizations about particular forest types are possible and estimates of  $NPP_f$  are made based on foliage biomass and FRT (e.g. Runyon et al., 1994). Given estimates of  $NPP_{Aw}$  and  $NPP_f$ , then allometric relationships of  $NPP_{Aw}$  to coarse root production, and  $NPP_f$  to fine root production, make possible an estimate of total NPP. New uncertainties have of course been added at each step and results would require significant validation based on whole ecosystem measurements of NPP. Nevertheless, these estimates of NPP would be relevant to validation of the MODIS NPP product which is based on a light use efficiency algorithm but does not specifically allocate NPP to wood, foliage and roots (Running et al., 1999).

## 5. Conclusions

Validation of regional to global estimates of NPP is a significant research challenge. The combination of lidar estimates of biomass and change detection estimates of stand age (the LCD approach) makes it possible to produce spatially extensive estimates of  $NPP_{Aw}$  over forested regions that are relevant to large scale validation efforts. In this study, the LCD approach was applied to estimate only  $NPP_{Aw}$  for relatively young stands in western OR, however, the on-going extension of the lidar and Landsat records will gradually increase the proportion of the forest land surface that can be analyzed.

## Acknowledgements

Thanks are due to Dick Waring, whose encouragement and enthusiasm was a key factor in motivating this analysis. This work was funded by the NASA Terrestrial Ecology Program (NRA-97-MTPE-08), through the Enhanced Thematic Mapper Plus Lidar for Forested Ecosystems (ETM+LIFE) Project, and by the U.S. Environmental Protection Agency STAR Program on Regional Scale Analysis and Assessment (Grant no. R828309).

## References

- Acker, S. A., Halpern, C. B., Harmon, M. E., & Dyrness, C. T. (2002). Trends in bole biomass accumulation, net primary production and tree mortality in *Pseudotsuga menziesii* forest of contrasting age. *Tree Physiology*, 22, 213–217.
- Asner, G. P. (2001). Cloud cover in Landsat observations of the Brazilian Amazon. *International Journal of Remote Sensing*, 22, 3855–3862.
- Bachelet, D., Neilson, R. P., Hickler, T., Drapek, R. J., Lenihan, J. M., Sykes, M. T., et al. (2003). Simulating past and future dynamics of natural ecosystems in the United States. *Global Biogeochemical Cycles*, 17(2) (14), 1–21.
- Blair, J. B., Coyle, D. B., Bufton, J. L., & Harding, D. J. (1994). Optimization of an airborne laser altimeter for remote sensing of vegetation and tree canopies. *Proceedings of the International Geosciences Remote Sensing Symposium* (pp. 939–941). Pasadena, CA: California Institute of Technology.
- Clark, D. A., Brown, S., Kicklighter, D. W., Chambers, J. Q., Thomlinson, J. R., & Ni, J. (2001). Measuring net primary productivity in forests: Concepts and field methods. *Ecological Applications*, 11(2), 356–370.
- Cohen, W. B., & Fiorella, M. (1998). Comparison of methods for detecting conifer forest change with Thematic Mapper imagery. In R. S. Lunetta, & C. D. Elvidge (Eds.), *Remote Sensing Change Detection, Environmental Monitoring Methods and Applications* (pp. 89–102). Chelsea, MI: Sleeping Bear Press Inc.
- Cohen, W. B., Fiorella, M., Gray, J., Helmer, E., & Anderson, K. (1998). An efficient and accurate method for mapping forest clearcuts in the Pacific Northwest using Landsat imagery. *Photogrammetric Engineering and Remote Sensing*, 64, 293–300.
- Cohen, W. B., Spies, T. A., Alig, R. J., Oetter, D. R., Maierperger, T. K., & Fiorella, M. (2002). Characterizing 23 years (1972–95) of stand replacement disturbance in western Oregon forests with Landsat imagery. *Ecosystems*, 5(2), 122–137.
- Crist, E. P., & Cicone, R. C. (1984). A physically-based transformation of thematic mapper data—the TM tasseled cap. *IEEE Transactions on Geoscience and Remote Sensing*, 22, 256–263.
- Curtis, P. S., Hanson, P. J., Barford, P., Randolph, J. C., Schmid, H. P., & Wilson, K. B. (2002). Biometric and eddy-covariance based estimates of annual carbon storage in five eastern North American deciduous forests. *Agricultural and Forest Meteorology*, 113, 3–19.
- Drake, J. B., Dubayah, R. O., Clark, D. B., Knox, R. G., Blair, J. B., Hofton, M. A., et al. (2002). Estimation of tropical forest structural characteristics using large-footprint lidar. *Remote Sensing of Environment*, 79, 305–319.
- Franklin, J. (2002). Dendrometer studies for stand volume and height measurements: Long-Term Ecological Research. Corvallis, OR: Forest Science Data Bank: TV009. [Database]. <http://www.fsl.orst.edu/iter/data/abstract.cfm?dbcode=TV009>. (4 December 2003)
- Franklin, J. F., & Dyrness, C. T. (1988). *Natural Vegetation of Oregon and Washington*. Corvallis: Oregon State University Press.
- Goetz, S., Prince, S. E., Goward, S. N., Thawley, M. M., Small, J., & Johnston, A. (1999). Mapping net primary production and related biophysical variables with remote sensing, application to the BOREAS region. *Journal of Geophysical Research*, 104, 27719–27734.
- Gower, S. T., Kucharik, C. J., & Norman, J. M. (1999). Direct and indirect estimation of leaf area index, fAPAR, and net primary production of terrestrial ecosystems. *Remote Sensing of Environment*, 70, 29–51.
- Hanson, E. J., Azuma, D. L., Hiserote, B. A. (2002). Site Index Equations and Mean Annual Increment Equations for Pacific Northwest Research Station Inventory and Analysis Inventories, 1985–2001. Pages 24. USDA Forest Service, PNW Research Station.
- Harding, D. J., Lefsky, M. A., & Parker, G. G. (2001). Lidar altimeter measurements of canopy structure: Methods and validation for closed-canopy broadleaf forest. *Remote Sensing of Environment*, 76, 283–297.

- Jenkins, J. C., Birdsey, R. A., & Pan, Y. (2001). Biomass and NPP estimation for the Mid-Atlantic region (USA) using plot-level forest inventory data. *Ecological Applications*, *11*, 1174–1193.
- Kauth, R. J., & Thomas, G. S. (1976). The tasselled cap—a graphic description of the spectral–temporal development of agricultural crops as seen by Landsat. *Lab. App. Remote Sens.*, vol. 4B (pp. 41–51). West Lafayette, IN: Purdue U.
- Landsberg, J. J., & Waring, R. H. (1997). A generalized model of forest productivity using simplified concepts of radiation-use efficiency, carbon balance, and partitioning. *Forest Ecology and Management*, *95*, 209–228.
- Law, B. E., Turner, D., Campbell, J., Sun, O., Van Tuyl, S., Ritts, W. D., et al. (2004). Disturbance and climate effects on carbon stocks and fluxes across western Oregon USA. *Global Change Biology*, *10*, 1–16.
- Lefsky, M. A., Cohen, W. B., Harding, D. J., Parker, G. G., Acker, S. A., & Gower, S. T. (2002). Lidar remote sensing of aboveground biomass in three biomes. *Global Ecology and Biogeography*, *11*(5), 393–400.
- Lefsky, M. A., Cohen, W. B., Acker, S. A., Spies, T. A., Parker, G. G., & Harding, D. (1999a). Lidar remote sensing of biophysical properties and canopy structure of forest of Douglas-fir and western hemlock. *Remote Sensing of Environment*, *70*, 339–361.
- Lefsky, M. A., Harding, D., Cohen, W. B., & Parker, G. G. (1999b). Surface lidar remote sensing of basal area and biomass in deciduous forests of eastern Maryland, USA. *Remote Sensing of Environment*, *67*, 83–98.
- Lefsky, M.A., Hudak, A.T., Cohen, W.B., & Acker, S.A. (2005a). Patterns of covariance between forest stand and canopy structure in the Pacific Northwest. *Remote Sensing of Environment*, *95*, 517–531.
- Lefsky, M.A., Hudak, A.T., Cohen, W.B., & Acker, S.A. (2005b). Geographic variability in lidar predictions of forest stand structure in the Pacific Northwest. *Remote Sensing of Environment*, *95*, 532–548.
- MacArthur, R. H., & Horn, H. S. (1969). Foliage profile by vertical measurements. *Ecology*, *50*, 802–804.
- Means, J. E., Acker, S. A., Harding, D. J., Blair, J. B., Lefsky, M. A., Cohen, W. B., et al. (1999). Use of large-footprint scanning airborne lidar to estimate forest stand characteristics in the western Cascades of Oregon. *Remote Sensing of Environment*, *67*, 298–308.
- Moer, M., & Stage, A. (1995). Most similar neighbor: An improved sample inference procedure for natural resource planning. *Forest Science*, *41*(2), 337–359.
- Nelson, R. F., Kimes, D. S., Salas, W. A., & Routhier, M. (2000). Secondary forest age and tropical forest biomass estimation using thematic mapper imagery. *BioScience*, *50*(5), 419–431.
- Ohmann, J. L., & Gregory, M. J. (2002). Predictive mapping of forest composition and structure with direct gradient analysis and nearest neighbor imputation in coastal Oregon, USA. *Canadian Journal of Forest Research*, *32*, 725–741.
- Pickett, S. T. A. (1989). Space-for-time substitution as an alternative to long-term studies. In G. E. Likens (Ed.), *Long-term Studies in Ecology* (pp. 110–135). Springer-Verlag.
- Reich, P. B., Koike, T., Gower, S. T., & Schoettle, A. W. (1995). Causes and consequences of variation in conifer leaf life-span. In W. K. Smith, & T. M. Hinkley (Eds.), *Ecophysiology of Coniferous Forests* (pp. 225–254). San Diego: Academic Press.
- Running, S. R., Baldocchi, D. D., Turner, D. P., Gower, S. T., Bakwin, P. S., & Hibbard, K. A. (1999). A global terrestrial monitoring network integrating tower fluxes, flask sampling, ecosystem modeling and EOS satellite data. *Remote Sensing of Environment*, *70*, 108–128.
- Running, S. W., & Hunt, E. R., Jr. (1993). Generalization of a forest ecosystem process model for other biomes, BIOME-BGC and an application for global scale models. In J. R. Ehleringer, & C. Fields (Eds.), *Scaling Physiological Processes: Leaf to Globe* (pp. 141–158). Orlando, FL: Academic Press.
- Runyon, J., Waring, R. H., Goward, S. N., & Welles, J. M. (1994). Environmental limits on net primary production and light use efficiency across the Oregon transect. *Ecological Applications*, *4*, 226–237.
- Ryan, M. G., Binkley, D., & Fownes, J. H. (1997). Age-related decline in forest productivity: Pattern and process. *Advances in Ecological Research*, *27*, 313–362.
- Schumacher, F. X., & Hall, F. D. S. (1933). Logarithmic expression of timber-tree volume. *Journal of Agricultural Research*, *47*, 719–734.
- Thornton, P. E. (1998). Regional ecosystem simulation: Combining surface- and satellite-based observations to study linkages between terrestrial energy and mass budgets, PhD dissertation. University of Montana, 280 pp.
- Thornton, P. E., Hasenauer, H., & White, M. A. (2000). Simultaneous estimation of daily solar radiation and humidity from observed temperature and precipitation: An application over complex terrain in Austria. *Agricultural and Forest Meteorology*, 255–271.
- Thornton, P. E., Law, B. E., Gholz, H. L., Clark, K. L., Falge, E., Ellsworth, D. S., et al. (2002). Modeling and measuring the effects of disturbance history and climate on carbon and water budgets in evergreen needleleaf forests. *Agricultural and Forest Meteorology*, *113*, 185–222.
- Thornton, P. E., & Running, S. W. (1999). An improved algorithm for estimating incident daily solar radiation from measurements of temperature, humidity, and precipitation. *Agricultural and Forest Meteorology*, *93*, 211–228.
- Thornton, P. E., Running, S. W., & White, M. A. (1997). Generating surfaces of daily meteorological variables over large regions of complex terrain. *Journal of Hydrology*, *190*, 214–251.
- Turner, D. P., Guzy, M., Lefsky, M. A., VanTuyl, S., Sun, O., Daly, C., et al. (2003). Effects of land use and fine scale environmental heterogeneity on net ecosystem production over a temperate coniferous forest landscape. *Tellus. B*, *55*(2), 657–669.
- Turner, D. P., Guzy, M., Lefsky, M., Ritts, W., VanTuyl, S., & Law, B. E. (2004a). Monitoring forest carbon sequestration with remote sensing and carbon cycle modeling. *Environmental Management*, *33*, 457–466.
- Turner, D. P., Ollinger, S., Smith, M. L., Krankina, O., & Gregory, M. (2004b). Scaling net primary production to a MODIS footprint in support of earth observing system product validation. *International Journal of Remote Sensing*, *25*, 1961–1979.
- USDA Forest Products Laboratory. (1999). Wood handbook—Wood as an engineering material. Gen. Tech. Rep. FPL-GTR-113. Madison, WI: U.S. Department of Agriculture, Forest Service, Forest Products Laboratory. 463 pp.
- USDA Forest Service Forest Inventory and Analysis. (1992). Forest Service Resource Inventories: An Overview. Forest Inventory, Economics, and Recreation Research. Washington, DC: USDA Forest Service.
- Wallin, D. O., Swanson, F. J., Marks, B., Cissel, J. H., & Kertis, J. (1996). Comparison of managed and pre-settlement landscape dynamics in forests of the Pacific Northwest, USA. *Forest Ecology and Management*, *85*, 291–309.